Cerebral blood volume in Alzheimer's disease and correlation with tissue structural integrity

Jinsoo Uh[a], **Kelly Lewis-Amezcua**[a], **Kristin Martin-Cook**[b], **Yamei Cheng**[a], **Myron Weiner**[b], **Ramon Diaz-Arrastia**[b], **Michael Devous Sr.**[b], **Dinggang Shen**[c], and **Hanzhang Lu**[a,*]

[a] Advanced Imaging Research Center, University of Texas Southwestern Medical Center, Dallas, TX 75390, United States

[b] Alzheimer's Disease Center, University of Texas Southwestern Medical Center, Dallas, TX 75390, United States

[c] Department of Radiology and Biomedical Research Imaging Center, University of North Carolina, Chapel Hill, NC 27599, United States

Abstract

A vascular component is increasingly recognized as important in Alzheimer's disease (AD). We measured cerebral blood volume (CBV) in patients with probable AD or Mild Cognitive Impairment (MCI) and in elderly non-demented subjects using a recently developed Vascular-Space-Occupancy (VASO) MRI technique. While both gray and white matters were examined, significant CBV deficit regions were primarily located in white matter, specifically in frontal and parietal lobes, in which CBV was reduced by 20% in the AD/MCI group. The regions with CBV deficit also showed reduced tissue structural integrity as indicated by increased apparent diffusion coefficients, whereas in regions without CBV deficits no such correlation was found. Subjects with lower CBV tended to have more white matter lesions in FLAIR MRI images and showed slower psychomotor speed. These data suggest that the vascular contribution in AD is primarily localized to frontal/parietal white matter and is associated with brain tissue integrity.

Keywords

Alzheimer's disease; Cerebral blood volume; Cerebral blood flow; VASO; MRI; Tissue integrity

1. Introduction

Alzheimer's disease (AD) is neurodegenerative disease associated with neuritic plaques composed of beta amyloid and neurofibrillary tangles composed of hyperphosphorylated *tau* protein. While amyloid/tau pathology is the primary focus in the field, recent evidence indicates that vascular factors are important in the pathogenesis of AD (de la Torre, 2004). This evidence comes from a wide spectrum of studies, including postmortem studies showing severe cerebral angiopathy in AD patients (Chui et al., 2006; Jagust et al., 2008; Tian et al., 2006), epidemiologic studies showing that many of the risk factors for AD are also associated with vascular disease (hypertension, hypercholesterolemia, diabetes, and hyperhomocysteinemia) (reviewed in de la Torre (2002)), and neuroimaging studies showing that AD patients have

greater volume of white matter hyperintensities of possible ischemic origin (Delano-Wood et al., 2008; Prins et al., 2004).

Brain vascular function can be assessed by several different methods. For in vivo studies, cerebral blood flow (CBF), the amount of blood reaching the tissue per unit time (Kety and Schmidt, 1948), is the most widely used parameter. Previous CBF studies in AD patients have found pronounced blood flow deficits in temporoparietal cortex, posterior cingulate cortex, and in some cases, frontal cortex (Alsop et al., 2000; Bartenstein et al., 1997; Ishii et al., 1997; Johnson et al., 2005; Kogure et al., 2000). CBF is known to be coupled to metabolic demand. Thus, although reduced CBF may be an indication of vascular dysfunction, it may also be simply due to lower metabolic demand in these regions (de Leon et al., 2001; Reiman et al., 2005; Small et al., 2000) in the face of relatively intact brain vasculature. In addition, CBF is also governed by many factors external to the brain, such as cardiac output, autonomic activity, and blood pressure. Therefore, it is necessary to study brain vasculature in AD with alternative vascular parameters.

Cerebral Blood Volume (CBV), the amount of blood per 100 ml of brain parenchyma, is an indicator of blood vessel lumen size and density. CBV has been less extensively studied than CBF, but was recently shown to be useful in assessing neovascularization in brain tumors (Law et al., 2004) and a good marker for angiogenesis and synaptogenesis (Pereira et al., 2007; Swain et al., 2003). In addition, the sensitivity of CBV to physiologic variation is about 38% of that of CBF (Grubb et al., 1974). Thus, CBV may be less dependent on the subject's depth and rate of respiration. We have recently developed a Vascular-Space-Occupancy (VASO) Magnetic Resonance Imaging (MRI) technique to quantitate CBV (Lu et al., 2005). In contrast with the Dynamic Susceptibility Contrast (DSC) MRI method, the VASO approach is based on steady-state signal and does not depend on arterial input function, which itself may be changed with disease. CBV measured by VASO shows a moderate correlation with that using DSC MRI, but also displays some deviations (Lu et al., 2005), suggesting that the two measures may have slightly different physiologic bases. The VASO technique also has the advantage that the sensitivity is sufficient to assess vascular health in white matter, which is ordinarily very difficult to assess due to very low vascularity.

In this study, we measured CBV in a group of patients with probable AD or Mild Cognitive Impairment (MCI), and identified regions with significant CBV decline compared to elderly non-demented controls. The relationship of CBV deficits to parenchymal damage was examined by correlating the regional CBV values to tissue water diffusion index as measured by diffusion tensor imaging (DTI), and the volume of white matter hyperintensities measured by FLAIR MRI. In addition, the CBV result was compared to neuropsychological test scores.

2. Methods

2.1. Participants

A group of probable AD/MCI patients ($n = 16$, 9M, 7F, age (years $\pm$ S.D.) = 70.7 $\pm$ 9.3) and a group of elderly controls ($n = 10$, 3M, 7F, age = 73.1 $\pm$ 4.4) were examined. The participants were recruited from the longitudinal cohorts maintained by the Alzheimer's Disease Center of University of Texas Southwestern Medical Center. The Health Insurance Portability and Accountability Act (HIPAA) compliant protocol was proved by the Institutional Review Board and written informed consent was obtained from all participants. Inclusion/exclusion criteria for all subjects were: (a) No contraindication to MRI scanning (pacemaker, implanted metallic objects, renal/liver disease), (b) general good health, with no serious or unstable medical conditions, (c) able and willing to provide informed consent (in the case of AD/MCI patients, caregivers co-signed consents), (d) age greater than 50, (e) no evidence of stroke in clinical MRI, and (f) Hachinski et al. (1975) score < 4. Additional criteria for the control group were

normal cognition and Clinical Dementia Rating (CDR; Morris, 1993) score = 0. Additional criteria for the AD/MCI group included a diagnosis of probable AD based on NINCDS/ADRDA criteria (McKhann et al., 1984) or a diagnosis of MCI based on Petersen criteria (Petersen et al., 1997) with CDR score = 0.5–1. In this study, we grouped the probable AD (8 subjects, CDR = 1) and MCI (8 subjects, CDR = 0.5) patients together because of the evidence that MCI is a potential pre-clinical form of AD (Petersen et al., 2001) and considerable overlap between these two diagnostic entities. Special caution was used to exclude any subjects with clinically obvious cerebrovacular disease (DeCarli et al., 2004), including a history of stroke, focal neurologic findings, or MRI evidence of cerebral infarction. The demographic information for the participants is summarized in Table 1.

2.2. MRI methods

The MRI investigatons were performed on a 3 T MR system (Philips Medical System, Best, The Netherlands). A body coil was used for radiofrequency (RF) transmission and an 8-channel head coil with parallel imaging capability was used for signal reception. We measured CBV maps using the VASO MRI technique that was developed by our laboratory (Lu et al., 2003, 2005). For the VASO imaging protocol, we used 32 coronal slices (voxel size 2 mm × 2 mm × 5 mm) to cover the entire brain. The other imaging parameters were: FOV = 192 mm × 192 mm, matrix size = 96 × 96, slice thickness = 5 mm, echo-planar-imaging (EPI) factor = 7, TR/TE = 6000 ms/3.4 ms, duration = 2.5 min. The inversion time, TI, was selected to be 1088 ms in accordance with the blood T1 estimate, 1624 ms (Lu et al., 2004). The scan protocol included a pre-contrast scan, injection of contrast agent by an MRI Power Injector (MEDRAD, Pittsburgh, PA) and a post-contrast scan. An FDA-approved contrast agent, Gd-DTPA (Magnevist®), was used with a standard dosage (0.1 mmol/kg). The post-contrast VASO scan was initiated 2 min after the injection to avoid signal fluctuations due to bolus passes.

In addition to the CBV images, a T1-weighted high resolution (1 mm × 1 mm × 1 mm) anatomical image using a magnetization-prepared rapid acquisition of gradient echo (MPRAGE) sequence (Brant-Zawadzki et al., 1992) was acquired for each subject for the use of brain normalization. We also acquired Diffusion Tensor Imaging (DTI) (TR/TE = 5281 ms/51 ms, FOV = 224 mm × 224 mm, resolution = 2 mm × 2 mm, 60 slices with thickness = 2 mm and gap = 1 mm) and Fluid-Attenuated Inversion Recovery (FLAIR) images (Essig et al., 1998) (TR/TI/TE = 11000 ms/2800 ms/ 125 ms, FOV = 230 mm × 230 mm, resolution = 0.45 mm × 0.45 mm, 24 slices with thickness = 5 mm and gap = 1 mm) for assessment of structural changes. The FLAIR scan was performed on 24 participants and all data were included in the analysis. The DTI scan was performed on 26 participants, but one subject showed significant motion artifact and was omitted from analysis. The DTI scan uses a single-shot spin echo EPI, and the diffusion encoding gradients have 30 directions based on the optimal scheme of Jones et al. (1999) with a b-factor of 1000 s/mm^2. The total scan duration was approximately 32 min.

Psychological testing results, including Mini-Mental State Exam (MMSE) (Folstein et al., 1975), Trail-making Tests A and B (Reitan, 1955), and the Consortium to Establish a Registry for Alzheimer's Disease (CERAD) battery (Morris et al., 1989), were available for comparison with the MRI data.

2.3. Data processing

Magnitude and phase MR images of the VASO scans were reconstructed on the scanner. The phase image was used to determine the sign of the magnetizations. The sign-corrected pre- and post-contrast VASO images were co-registered by Statistical Parametric Mapping (SPM2) and the CBV was calculated using an algorithm described previously (Lu et al., 2005):

$$\text{CBV} = \frac{S_{\text{post}} - S_{\text{pre}}}{M_0 C_{\text{b}}} \times 100 \ (\text{ml/100 ml brain}) \quad (1)$$

where S_{pre} and S_{post} are the MRI signals before and after the contrast agent injection, respectively, M_0 the MRI signal for a pure-water voxel at equilibrium magnetization, C_{b} is the water content of blood and is assumed to 0.87 ml water/ml blood (Herscovitch and Raichle, 1985). The M_0 for each subject is estimated from a proton-density weighted images (TR = 20000 ms, TE = 10 ms).

To spatially register the individual CBV maps into a standard brain template so that group comparison can be performed, we used the following steps (Fig. 1) to obtain a "normalized CBV" for each subject. The raw CBV map was co-registered (rigid-body registration) by SPM2 to the subject's T1-weighted anatomical image. The individual T1-weighted image was then registered (elastic registration) to a template T1 image. This step used an elastic registration algorithm, Hierarchical Attribute Matching Mechanism for Elastic Registration (HAMMER) proposed by Shen and Davatzikos (2002), which detects and corrects for region-specific brain atrophy (Davatzikos et al., 2001). This feature is important to ensure that the comparison truly reflects vascular parameters rather than brain volume reduction. Once the individual T1 image was registered to the template brain, the same geometric transformation was applied to the individual CBV map so that the CBV map is now also in the standard space. Finally, in order to remove the effect of global CBV variations across subjects and focus on regional differences between AD/MCI subjects and controls, we divided the CBV value of each voxel by the mean CBV value of the cerebellum. Cerebellum was chosen as the reference tissue because cerebellum is minimally affected in AD (Karbe et al., 1994).

For voxel-by-voxel analysis, the normalized CBV map was smoothed by a Gaussian filter with 12 mm full-width-at-half-maximum (FWHM) (Alsop et al., 2000; Ashburner and Friston, 2000; Johnson et al., 2005).We conducted a two sample t-test using SPM2 to identify clusters showing significant CBV deficit ($p < 0.005$, voxel cluster size $> 1250 \ \text{mm}^3$) (Xu et al., 2007). We also performed a manual region-of-interest (ROI) analysis based on the normalized images. The regions examined included frontal white matter, parietal white matter, occipital white matter, hippocampus, and parietotemporal gray matter. Circular ROIs of 6-mm (for parietotemporal gray matter) or 8-mm (for other regions) diameter were carefully positioned in different anatomic regions to calculate the regional CBV values. In addition, similar ROI analysis was performed on the individual images to test the reliability of the results.

Apparent diffusion coefficient (ADC) and fractional anisotropy (FA) were calculated from the DTI images using DTI studio (Johns Hopkins University, Baltimore, MD). ADC and FA maps were then normalized to the template space in the same way as described for the CBV maps. The hyperintensity voxels in FLAIR images were identified with a semi-automatic method (Marquez de la Plata et al., 2007). Briefly, the FLAIR images were skull-stripped and the voxels with signal intensity greater than 2 standard deviations above average were delineated as a preliminary mask. Next, the preliminary mask was manually edited to remove spurious voxels due to fat signal, motion effect, edge effect, or coil sensitivity inhomogeneity. The total volume within the final mask was quantified for each subject. For correlation analysis between CBV, diffusion parameters, and neuropsychological test scores, the CBV deficit clusters as defined from the voxel-based comparison were used as masks for spatial averaging. Pearson correlation coefficients were calculated to assess the significance of the correlation. We also calculated Spearman rank correlation to assess the possible influence of outlier points.

3. Results

Fig. 2a and b shows the averaged CBV maps of the AD/MCI and control groups, respectively. Fig. 3 shows a voxel-by-voxel group comparison. After applying statistical threshold ($p < 0.005$ for each voxel, cluster size > 1250 mm^3), the regions showing CBV decline were overlaid on the T1 weighted anatomic image. Significant CBV deficits were observed primarily in white matter, located bilaterally in frontal lobes and extending to parietal lobes (Fig. 3). No significant clusters were observed for the opposite contrast (i.e., CBV in AD/MCI group greater than CBV in controls). The voxel-based results are consistent with the manual ROI results, which showed that CBV in AD/MCI patients were 26.1% ($p < 0.001$) and 18.5% ($p = 0.015$) lower than in controls in frontal and parietal white matters, respectively (Fig. 4). This trend was also seen in occipital white matter, but the level of statistical significance was lower ($p = 0.04$). No significant difference was observed in parietotemporal gray matter and hippocampus. The ROI analysis performed on the individual images showed the similar results: The AD/MCI patients showed significant CBV deficit in the three white matter ROIs while no significant difference was observed in parietotemporal gray matter and hippocampus.

To assess the effect of CBV deficit on neural tissue integrity, diffusion parameters in regions showing CBV deficits were calculated. Fig. 5 shows a significant negative correlation (Pearson correlation $p = 0.021$, $r = 0.41$; Spearman rank correlation $p = 0.027$, $r = 0.39$) between apparent diffusion coefficient (ADC) and the CBV values across subjects, suggesting that subjects with lower CBV had higher diffusion coefficients. A higher ADC indicates that water molecules diffuse more freely, implying reduced tissue structural barrier due to axonal membrane and myelin damage. In order to further confirm that the observed ADC change is related to CBV decline and not a global phenomenon, we performed additional analysis in which another set of white matter voxels (with the same number of voxels) were selected based on the criterion of similar CBV between AD/MCI and controls (i.e., t-test statistic around 0). In these voxels, no correlation was found between CBV and ADC across subjects (Pearson correlation $p = 0.37$, $r = 0.07$; Spearman rank correlation $p = 0.28$, $r = 0.12$). We also performed correlation analysis between CBV and fractional anisotropy (FA), but did not find a significant correlation (Pearson correlation $p = 0.46$, $r = 0.02$; Spearman rank correlation $p = 0.36$, $r = 0.07$), suggesting that vascular insult to white matter can change the tissue diffusion coefficient but this change appears to be present in all directions (both parallel and perpendicular to the axon tracts).

Volume of white matter hyperintensities (WMH) on FLAIR image is another index of tissue damage. Fig. 6 plots the correlation between CBV and WMH volume. A weak correlation (Pearson correlation $p = 0.101$, $r = 0.27$; Spearman rank correlation $p = 0.049$, $r = 0.35$) can be seen, suggesting that subjects with lower CBV tend to have a greater volume of WMH. This relationship, however, barely reached statistical threshold and the data showed large dispersion. One possible reason is that WMH are also produced by non-vascular causes of neurodegeneration and inflammation (Kates et al., 1996).

We also examined the correlation between CBV and several neuropsychological tests including MMSE, Trail-making Tests A and B, and the CERAD battery. We found that the normalized CBV values correlated with impairment of performance on the Trails A test (Pearson correlation $p = 0.051$, $r = 0.34$; Spearman rank correlation $p = 0.094$, $r = 0.27$). The other tests also showed a trend of correlation (lower CBV corresponding to poor performance), but did not reach significance.

4. Discussion

We compared CBV in a group of patients with probable AD or MCI with CBV in an elderly control group. We found that CBV in these patients declines in frontal and parietal lobes;

primarily in white matter. The CBV changes are correlated with structural damage as measured by diffusion tensor imaging, which appears to be specific to CBV deficit regions and was not found in regions where CBV was normal. The structural consequences of the CBV deficit are further confirmed by WMH volume, which increased with lower CBV values. Finally, the lower CBV and the structural damage were associated with reduction of psychomotor speed.

The CBV deficit regions identified by this study suggest that frontal white matter is probably the most vulnerable tissue in terms of vascular contributions to AD and is consistent with the observation that cerebrovascular pathology affects frontal lobe functions (Nagata et al., 2000; Reed et al., 2000). In this regard, it is possible that the CBV deficit investigated in this study indicates the vascular contribution to the dementia of AD. Thus, it is likely that many AD patients have combined neurodegenerative and vascular pathology underlying the clinical manifestations of the disease. Given the common co-existence of these two components in the majority of patients, the characterization of vascular factor is important. The observation that CBV deficit regions are mainly in white matter may be associated with autoregulation differences between gray and white matter. Cerebral autoregulation is characterized by the response that, when perfusion pressure is low, the blood vessels (primarily arterioles and small arteries) can actively dilate to "attract" more blood to the tissue. Since gray matter has greater vascularities, it is likely to have higher autoregulatory capacity. The white matter, on the other hand, only has about 1/3 of the blood vessels, therefore may deplete its autoregulatory capacity before gray matter.

Recent studies support that vascular dysfunction in frontal lobe is of significant relevance in the pathogenesis of AD. Nishimura et al. (2007) performed a longitudinal study in which perfusion deficits in frontal and temporoparietal lobes were measured and the disease progression was monitored using serial MMSE scores. They found that frontal lobe deficit (at baseline) was more predictive of future cognitive decline than were temporoparietal regions. Another recent study on transgenic mouse models (Meyer et al., 2008) has reported that vascular alteration in AD is not simply a generalized reduction of vascular density, but instead involves significant uneven redistribution/remodeling of vascular networks. This can potentially decouple CBV and CBF. The authors have further mapped the spatial specificity of the vascular abnormalities and noted that the deficits prominently clustered in the frontal cortex as well as temporal cortices.

Many previous studies have examined CBF deficit in AD and identified temporoparietal cortex and posterior cingulate cortex as the primary affected regions in AD (Alsop et al., 2000; Bartenstein et al., 1997; Ishii et al., 1997; Johnson et al., 2005; Kogure et al., 2000), differing from findings in the present study. One possible reason for the discrepancy is that CBF can be affected by other factors such as metabolic demand. This notion is supported by the observations that the CBF deficit regions, e.g. posterior cingulate cortex, hippocampus, also show a deficit in glucose metabolism as measured by FDG-PET (Mosconi et al., 2005; Perneczky et al., 2007). Thus, CBF reduction may not be due to brain vascular dysfunction, but could be related solely to lower metabolic demand/neural activity. Another possible reason is that the AD/MCI group recruited for this study is at an early stage (mean MMSE = 26.6) while those of the studies reporting significant CBF deficit are at a later stage. For example, Alsop et al. (2000) used AD subjects with a mean MMSE score of 20.8. In a study that examined similar stage of patients (mean MMSE = 27.7) (Johnson et al., 2005), no significant CBF deficit in white matter was found, but in our study, an MR contrast agent was used to enhance the sensitivity, which might have allowed the detection of deficit in white matter. A few previous studies have also examined vascular dysfunction in AD using CBV measures derived from DSC MRI (Bozzao et al., 2001; Gonzalez et al., 1995; Harris et al., 1998; Maas et al., 1997). Although a moderate CBV deficit was noted in temporoparietal cortex when using a relatively low threshold of $p < 0.05$ (Harris et al., 1998), these studies did not correct for regional atrophy

during the CBV comparison. In view of pronounced temporal lobe atrophy commonly observed in AD patients (Thompson et al., 2003), the CBV differences may be, at least partly, attributed to the tissue volume loss, as also noted by the authors (Harris et al., 1998). A second possible reason is that the CBV measures derived from DSC MRI may actually contain some contributions from CBF, due to the use of arterial input function in the DSC data processing (Ostergaard et al., 1996).

We have also specifically examined the CBV values in medial temporal lobe (MTL), the primary site of brain atrophy and amyloid plaque deposition, using both voxel-based analysis and ROI-based analysis. We did not observe a CBV decrease or a trend of decrease in MTL, indicating that vascular insult is not a major factor in this region for the subjects recruited for this study. This result supports the notion that MTL pathology in AD is not vascular in origin. Furthermore, given the repeated observation that plaque and tangle accumulation begins in MTL and only later affects parietal lobe and frontal lobes (Thompson et al., 2003), our observation of frontal lobe-dominant CBV deficit in AD/MCI patients suggests that the neurodegenerative and vascular pathologies in AD may be two separate processes. However, it should be noted that a recent in vivo mapping of amyloid deposition has shown greater deposition in frontal lobe than in the MTL (Buckner et al., 2005).

We were surprised that lower scores on Trails A, an assessment of psychomotor speed, showed correlation with our measures of vascular dysfunction while the tests more sensitive to cognitive impairment (Trails B and the CERAD Battery) did not. However, given our finding of predominantly white-matter-specific CBV deficits, this result is consistent with the notion that white matter integrity is critical for the speed of neuronal transmission. On the other hand, cognitively demanding tasks such as Trails B and CERAD require more gray matter processing and gray matter has more CBV reserve. Thus the correlations between these tasks and the CBV measures were not strong.

5. Conclusion

Vascular factors may contribute to the pathogenesis of AD. While both gray and white matter were examined, significant CBV deficit regions were primarily located in the white matter of the frontal and parietal lobes, in which CBV was reduced by ~20% in the patient group. These CBV deficits correlated with parenchymal damage as assessed by diffusion tensor imaging and FLAIR MRI. In addition, the amount of CBV deficit also appeared to correlate with impairment of psychomotor speed.

Acknowledgments

References

Alsop DC, Detre JA, Grossman M. Assessment of cerebral blood flow in Alzheimer's disease by spin-labeled magnetic resonance imaging. Ann Neurol 2000;47:93–100. [PubMed: 10632106]

Ashburner J, Friston KJ. Voxel-based morphometry—the methods. Neuroimage 2000;11:805–821. [PubMed: 10860804]

Bartenstein P, Minoshima S, Hirsch C, Buch K, Willoch F, Mosch D, Schad D, Schwaiger M, Kurz A. Quantitative assessment of cerebral blood flow in patients with Alzheimer's disease by SPECT. J Nucl Med 1997;38:1095–1101. [PubMed: 9225797]

Bozzao A, Floris R, Baviera ME, Apruzzese A, Simonetti G. Diffusion and perfusion MR imaging in cases of Alzheimer's disease: correlations with cortical atrophy and lesion load. AJNR Am J Neuroradiol 2001;22:1030–1036. [PubMed: 11415893]

Brant-Zawadzki M, Gillan GD, Nitz WR. MP RAGE: a three-dimensional, T1-weighted, gradient-echo sequence—initial experience in the brain. Radiology 1992;182:769–775. [PubMed: 1535892]

Buckner RL, Snyder AZ, Shannon BJ, LaRossa G, Sachs R, Fotenos AF, Sheline YI, Klunk WE, Mathis CA, Morris JC, Mintun MA. Molecular, structural, and functional characterization of Alzheimer's disease: evidence for a relationship between default activity, amyloid, and memory. J Neurosci 2005;25:7709–7717. [PubMed: 16120771]

Chui HC, Zarow C, Mack WJ, Ellis WG, Zheng L, Jagust WJ, Mungas D, Reed BR, Kramer JH, Decarli CC, Weiner MW, Vinters HV. Cognitive impact of subcortical vascular and Alzheimer's disease pathology. Ann Neurol 2006;60:677–687. [PubMed: 17192928]

Davatzikos C, Genc A, Xu D, Resnick SM. Voxel-based morphometry using the RAVENS maps: methods and validation using simulated longitudinal atrophy. Neuroimage 2001;14:1361–1369. [PubMed: 11707092]

de la Torre JC. Alzheimer disease as a vascular disorder: nosological evidence. Stroke 2002;33:1152–1162. [PubMed: 11935076]

de la Torre JC. Is Alzheimer's disease a neurodegenerative or a vascular disorder? Data, dogma, and dialectics. Lancet Neurol 2004;3:184–190. [PubMed: 14980533]

de Leon MJ, Convit A, Wolf OT, Tarshish CY, DeSanti S, Rusinek H, Tsui W, Kandil E, Scherer AJ, Roche A, Imossi A, Thorn E, Bobinski M, Caraos C, Lesbre P, Schlyer D, Poirier J, Reisberg B, Fowler J. Prediction of cognitive decline in normal elderly subjects with 2-[(18)F]fluoro-2-deoxy-D-glucose/poitron-emission tomography (FDG/PET). Proc Natl Acad Sci USA 2001;98:10966–10971. [PubMed: 11526211]

DeCarli C, Mungas D, Harvey D, Reed B, Weiner M, Chui H, Jagust W. Memory impairment, but not cerebrovascular disease, predicts progression of MCI to dementia. Neurology 2004;63:220–227. [PubMed: 15277612]

Delano-Wood L, Abeles N, Sacco JM, Wierenga CE, Horne NR, Bozoki A. Regional white matter pathology in mild cognitive impairment: differential influence of lesion type on neuropsychological functioning. Stroke 2008;39:794–799. [PubMed: 18258826]

Essig M, Hawighorst H, Schoenberg SO, Engenhart-Cabillic R, Fuss M, Debus J, Zuna I, Knopp MV, van Kaick G. Fast fluid-attenuated inversion-recovery (FLAIR) MRI in the assessment of intraaxial brain tumors. J Magn Reson Imaging 1998;8:789–798. [PubMed: 9702879]

Folstein MF, Folstein SE, McHugh PR. "Mini-mental state" A practical method for grading the cognitive state of patients for the clinician. J Psychiatr Res 1975;12:189–198. [PubMed: 1202204]

Gonzalez RG, Fischman AJ, Guimaraes AR, Carr CA, Stern CE, Halpern EF, Growdon JH, Rosen BR. Functional MR in the evaluation of dementia: correlation of abnormal dynamic cerebral blood volume measurements with changes in cerebral metabolism on positron emission tomography with fludeoxyglucose F 18. AJNR Am J Neuroradiol 1995;16:1763–1770. [PubMed: 8693972]

Grubb RL Jr, Raichle ME, Eichling JO, Ter-Pogossian MM. The effects of changes in $PaCO_2$ on cerebral blood volume, blood flow, and vascular mean transit time. Stroke 1974;5:630–639. [PubMed: 4472361]

Hachinski VC, Iliff LD, Zilhka E, Du Boulay GH, McAllister VL, Marshall J, Russell RW, Symon L. Cerebral blood flow in dementia. Arch Neurol 1975;32:632–637. [PubMed: 1164215]

Harris GJ, Lewis RF, Satlin A, English CD, Scott TM, Yurgelun-Todd DA, Renshaw PF. Dynamic susceptibility contrast MR imaging of regional cerebral blood volume in Alzheimer disease: a promising alternative to nuclear medicine. AJNR Am J Neuroradiol 1998;19:1727–1732. [PubMed: 9802497]

Herscovitch P, Raichle ME. What is the correct value for the brain–blood partition coefficient for water? J Cereb Blood Flow Metab 1985;5:65–69. [PubMed: 3871783]

Ishii K, Sasaki M, Yamaji S, Sakamoto S, Kitagaki H, Mori E. Demonstration of decreased posterior cingulate perfusion in mild Alzheimer's disease by means of H215O positron emission tomography. Eur J Nucl Med 1997;24:670–673. [PubMed: 9169576]

Jagust WJ, Zheng L, Harvey DJ, Mack WJ, Vinters HV, Weiner MW, Ellis WG, Zarow C, Mungas D, Reed BR, Kramer JH, Schuff N, DeCarli C, Chui HC. Neuropathological basis of magnetic resonance images in aging and dementia. Ann Neurol 2008;63:72–80. [PubMed: 18157909]

Johnson NA, Jahng GH, Weiner MW, Miller BL, Chui HC, Jagust WJ, Gorno-Tempini ML, Schuff N. Pattern of cerebral hypoperfusion in Alzheimer disease and mild cognitive impairment measured with arterial spin-labeling MR imaging: initial experience. Radiology 2005;234:851–859. [PubMed: 15734937]

Jones DK, Horsfield MA, Simmons A. Optimal strategies for measuring diffusion in anisotropic systems by magnetic resonance imaging. Magn Reson Med 1999;42:515–525. [PubMed: 10467296]

Karbe H, Kertesz A, Davis J, Kemp BJ, Prato FS, Nicholson RL. Quantification of functional deficit in Alzheimer's disease using a computer-assisted mapping program for 99mTc-HMPAO SPECT. Neuroradiology 1994;36:1–6. [PubMed: 8107986]

Kates R, Atkinson D, Brant-Zawadzki M. Fluid-attenuated inversion recovery (FLAIR): clinical prospectus of current and future applications. Top Magn Reson Imaging 1996;8:389–396. [PubMed: 9402679]

Kety SS, Schmidt CF. The nitrous oxide method for the quantitative determination of cerebral blood flow in man: theory, procedure and normal values. J Clin Invest 1948;27:476–483.

Kogure D, Matsuda H, Ohnishi T, Asada T, Uno M, Kunihiro T, Nakano S, Takasaki M. Longitudinal evaluation of early Alzheimer's disease using brain perfusion SPECT. J Nucl Med 2000;41:1155–1162. [PubMed: 10914904]

Law M, Yang S, Babb JS, Knopp EA, Golfinos JG, Zagzag D, Johnson G. Comparison of cerebral blood volume and vascular permeability from dynamic susceptibility contrast-enhanced perfusion MR imaging with glioma grade. AJNR Am J Neuroradiol 2004;25:746–755. [PubMed: 15140713]

Lu H, Clingman C, Golay X, van Zijl PC. Determining the longitudinal relaxation time (T1) of blood at 3.0 T. Magn. Reson Med 2004;52:679–682.

Lu H, Golay X, Pekar JJ, Van Zijl PC. Functional magnetic resonance imaging based on changes in vascular space occupancy. Magn Reson Med 2003;50:263–274. [PubMed: 12876702]

Lu H, Law M, Johnson G, Ge Y, van Zijl PC, Helpern JA. Novel approach to the measurement of absolute cerebral blood volume using vascular-space-occupancy magnetic resonance imaging. Magn Reson Med 2005;54:1403–1411. [PubMed: 16254955]

Maas LC, Harris GJ, Satlin A, English CD, Lewis RF, Renshaw PF. Regional cerebral blood volume measured by dynamic susceptibility contrast MR imaging in Alzheimer's disease: a principal components analysis. J Magn Reson Imaging 1997;7:215–219. [PubMed: 9039618]

Marquez de la Plata C, Ardelean A, Koovakkattu D, Srinivasan P, Miller A, Phuong V, Harper C, Moore C, Whittemore A, Madden C, Diaz-Arrastia R, Devous M Sr. Magnetic resonance imaging of diffuse axonal injury: quantitative assessment of white matter lesion volume. J Neurotrauma 2007;24:591–598. [PubMed: 17439343]

McKhann G, Drachman D, Folstein M, Katzman R, Price D, Stadlan EM. Clinical diagnosis of Alzheimer's disease: report of the NINCDS-ADRDA Work Group under the auspices of Department of Health and Human Services Task Force on Alzheimer's Disease. Neurology 1984;34:939–944. [PubMed: 6610841]

Meyer EP, Ulmann-Schuler A, Staufenbiel M, Krucker T. Altered morphology and 3D architecture of brain vasculature in a mouse model for Alzheimer's disease. Proc Natl Acad Sci USA 2008;105:3587–3592. [PubMed: 18305170]

Morris JC. The Clinical Dementia Rating (CDR): current version and scoring rules. Neurology 1993;43:2412–2414. [PubMed: 8232972]

Morris JC, Heyman A, Mohs RC, Hughes JP, van Belle G, Fillenbaum G, Mellits ED, Clark C. The Consortium to Establish a Registry for Alzheimer's Disease (CERAD). Part I. Clinical and neuropsychological assessment of Alzheimer's disease. Neurology 1989;39:1159–1165. [PubMed: 2771064]

Mosconi L, Tsui WH, De Santi S, Li J, Rusinek H, Convit A, Li Y, Boppana M, de Leon MJ. Reduced hippocampal metabolism in MCI and AD: automated FDG-PET image analysis. Neurology 2005;64:1860–1867. [PubMed: 15955934]

Nagata K, Maruya H, Yuya H, Terashi H, Mito Y, Kato H, Sato M, Satoh Y, Watahiki Y, Hirata Y, Yokoyama E, Hatazawa J. Can PET data differentiate Alzheimer's disease from vascular dementia? Ann NY Acad Sci 2000;903:252–261. [PubMed: 10818514]

Nishimura T, Hashikawa K, Fukuyama H, Kubota T, Kitamura S, Matsuda H, Hanyu H, Nabatame H, Oku N, Tanabe H, Kuwabara Y, Jinnouchi S, Kubol A. Decreased cerebral blood flow and prognosis of Alzheimer's disease: a multicenter HMPAO-SPECT study. Ann Nucl Med 2007;21:15–23. [PubMed: 17373332]

Ostergaard L, Weisskoff RM, Chesler DA, Gyldensted C, Rosen BR. High resolution measurement of cerebral blood flow using intravascular tracer bolus passages. Part I. Mathematical approach and statistical analysis. Magn Reson Med 1996;36:715–725. [PubMed: 8916022]

Pereira AC, Huddleston DE, Brickman AM, Sosunov AA, Hen R, McKhann GM, Sloan R, Gage FH, Brown TR, Small SA. An in vivo correlate of exercise-induced neurogenesis in the adult dentate gyrus. Proc Natl Acad Sci USA 2007;104:5638–5643. [PubMed: 17374720]

Perneczky R, Hartmann J, Grimmer T, Drzezga A, Kurz A. Cerebral metabolic correlates of the clinical dementia rating scale in mild cognitive impairment. J Geriatr Psychiatry Neurol 2007;20:84–88. [PubMed: 17548777]

Petersen RC, Doody R, Kurz A, Mohs RC, Morris JC, Rabins PV, Ritchie K, Rossor M, Thal L, Winblad B. Current concepts in mild cognitive impairment. Arch Neurol 2001;58:1985–1992. [PubMed: 11735772]

Petersen RC, Smith GE, Waring SC, Ivnik RJ, Kokmen E, Tangelos EG. Aging, memory, and mild cognitive impairment. Int Psychogeriatr 1997;9(Suppl. 1):65–69. [PubMed: 9447429]

Prins ND, van Dijk EJ, den Heijer T, Vermeer SE, Koudstaal PJ, Oudkerk M, Hofman A, Breteler MM. Cerebral white matter lesions and the risk of dementia. Arch Neurol 2004;61:1531–1534. [PubMed: 15477506]

Reed BR, Eberling JL, Mungas D, Weiner MW, Jagust WJ. Memory failure has different mechanisms in subcortical stroke and Alzheimer's disease. Ann Neurol 2000;48:275–284. [PubMed: 10976633]

Reiman EM, Chen K, Alexander GE, Caselli RJ, Bandy D, Osborne D, Saunders AM, Hardy J. Correlations between apolipoprotein E epsilon4 gene dose and brain-imaging measurements of regional hypometabolism. Proc Natl Acad Sci USA 2005;102:8299–8302. [PubMed: 15932949]

Reitan RM. The relation of the trail making test to organic brain damage. J Consult Psychol 1955;19:393–394. [PubMed: 13263471]

Shen D, Davatzikos C. HAMMER: hierarchical attribute matching mechanism for elastic registration. IEEE Trans Med Imaging 2002;21:1421–1439. [PubMed: 12575879]

Small GW, Ercoli LM, Silverman DH, Huang SC, Komo S, Bookheimer SY, Lavretsky H, Miller K, Siddarth P, Rasgon NL, Mazziotta JC, Saxena S, Wu HM, Mega MS, Cummings JL, Saunders AM, Pericak-Vance MA, Roses AD, Barrio JR, Phelps ME. Cerebral metabolic and cognitive decline in persons at genetic risk for Alzheimer's disease. Proc Natl Acad Sci USA 2000;97:6037–6042. [PubMed: 10811879]

Swain RA, Harris AB, Wiener EC, Dutka MV, Morris HD, Theien BE, Konda S, Engberg K, Lauterbur PC, Greenough WT. Prolonged exercise induces angiogenesis and increases cerebral blood volume in primary motor cortex of the rat. Neuroscience 2003;117:1037–1046. [PubMed: 12654355]

Thompson PM, Hayashi KM, de Zubicaray G, Janke AL, Rose SE, Semple J, Herman D, Hong MS, Dittmer SS, Doddrell DM, Toga AW. Dynamics of gray matter loss in Alzheimer's disease. J Neurosci 2003;23:994–1005. [PubMed: 12574429]

Tian J, Shi J, Smallman R, Iwatsubo T, Mann DM. Relationships in Alzheimer's disease between the extent of Abeta deposition in cerebral blood vessel walls, as cerebral amyloid angiopathy, and the amount of cerebrovascular smooth muscle cells and collagen. Neuropathol Appl Neurobiol 2006;32:332–340. [PubMed: 16640651]

Xu G, Antuono PG, Jones J, Xu Y, Wu G, Ward D, Li SJ. Perfusion fMRI detects deficits in regional CBF during memory-encoding tasks in MCI subjects. Neurology 2007;69:1650–1656. [PubMed: 17954780]
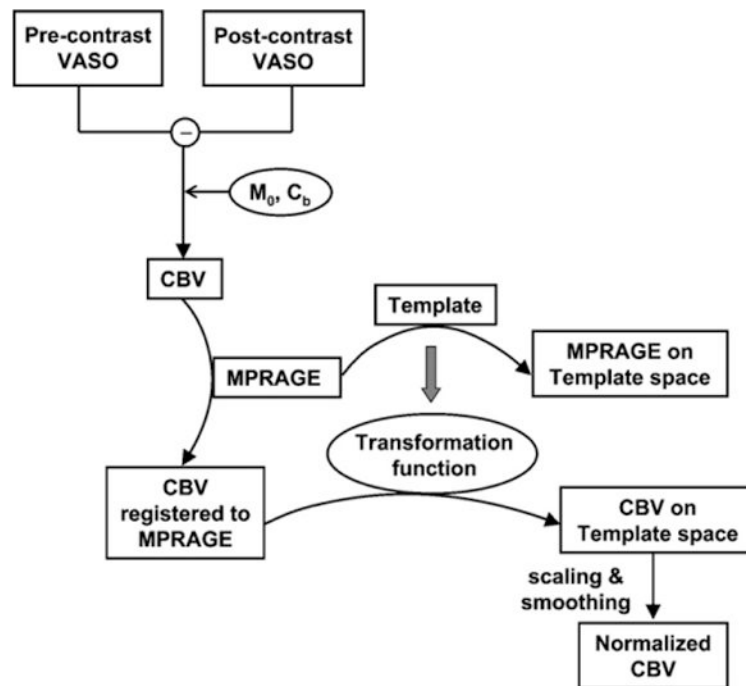
Fig. 1.
Procedure for the calculation of normalized CBV. The signal differences between pre- and post-contrast VASO images were first calculated, which was realigned to the T1-weighted anatomic image. The image of each individual was then registered to the brain template using an elastic transformation. The CBV value of each voxel was normalized to the cerebellum CBV to reduce the effect of normal variations in global CBV.
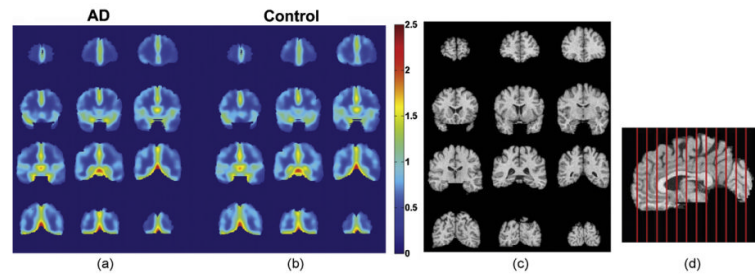
Fig. 2.
Group averaged CBV maps in AD/MCI and control subjects. (a) Relative CBV maps in AD/MCI patients. (b) Relative CBV maps in controls. The scale of the color bar is from 0 to 2.5 times the cerebellum CBV. (c) An anatomical image corresponding to the slices presented. (d) The locations of coronal slices are marked in a sagittal anatomical image. (For interpretation of the references to color in this figure legend, the reader is referred to the web version of the article.)
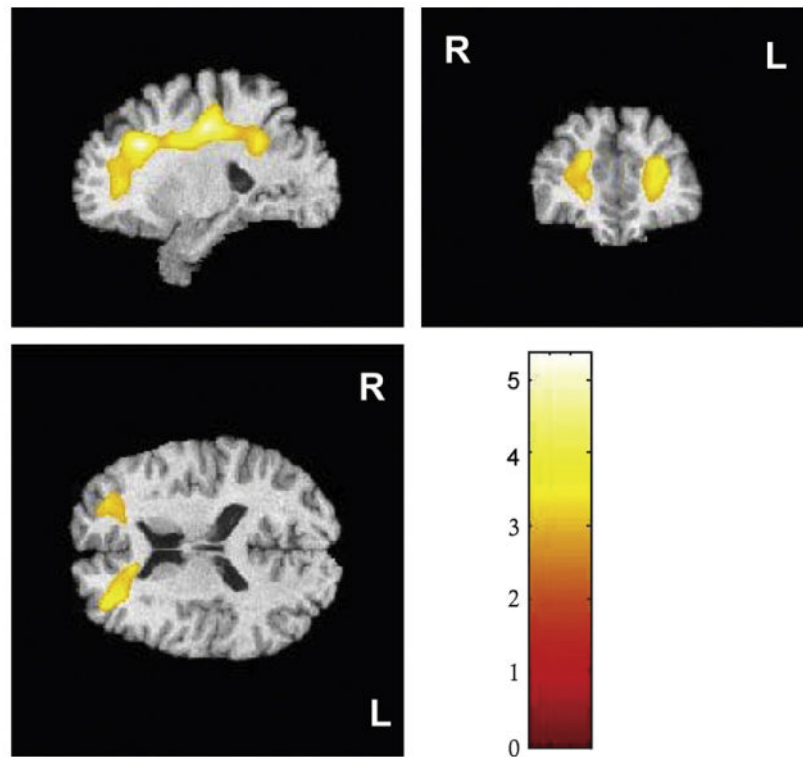
Fig. 3.
Results of voxel-based analysis with two sample *t*-test on the CBV maps of AD/MCI and control groups. The colored regions show significant CBV deficit in AD/MCI patients (*p* < 0.005 and minimum cluster size = 1250 mm^3). The color bar indicates Student's *t*-statistic value. (For interpretation of the references to color in this figure legend, the reader is referred to the web version of the article.)
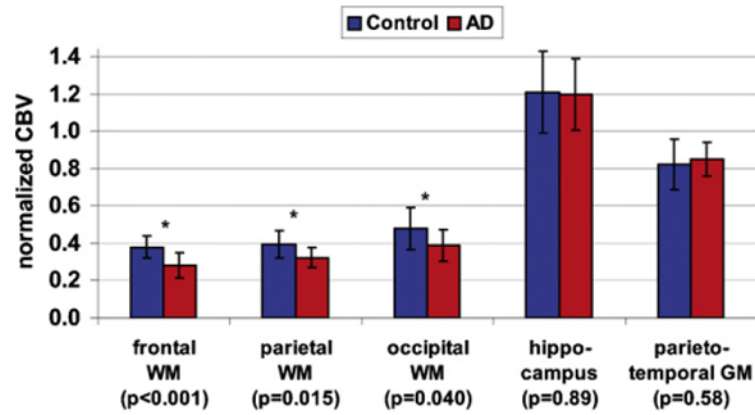
Fig. 4.
ROI analysis results of CBV in AD/MCI and control groups. 8-mm (frontal, parietal, and occipital WM, hippocampus) or 6-mm (parietotemporal GM) diameter circles were drawn on each subject's normalized CBV maps to obtain the mean value for each ROI. The asterisks indicate regions with significant differences (two sample Student's *t*-test, $p < 0.05$).
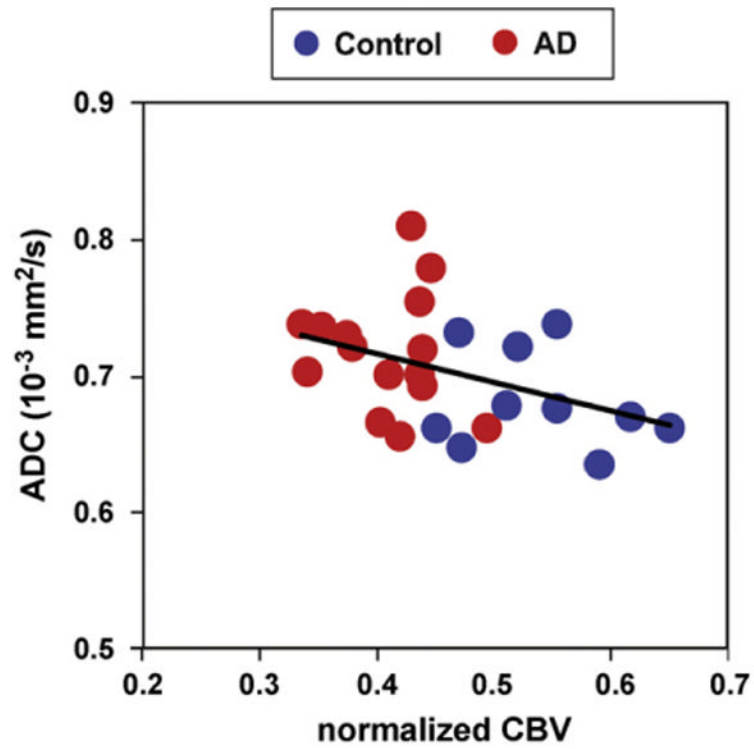
Fig. 5.
Correlation between CBV and ADC values across subjects (including both AD/MCI patients and controls, $n = 25$). The values of CBV and ADC for each subject were calculated from the regions showing significant CBV deficits (see Fig. 3).
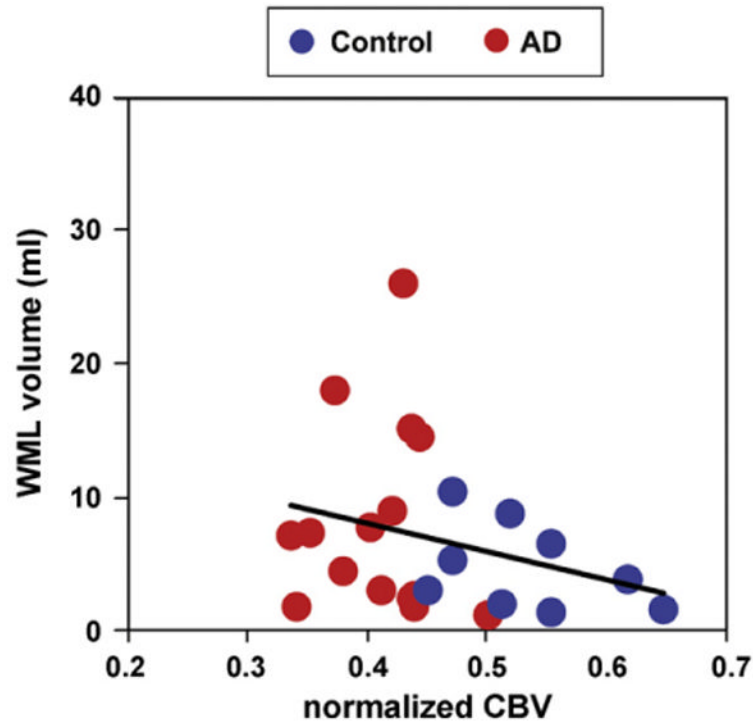
Fig. 6.
Correlation between the normalized CBV and the volume of white matter lesion measured by FLAIR images (including both AD/MCI patients and controls, $n = 24$). The value of CBV for each subject was calculated from the regions showing significant CBV deficits, and the volume of white matter lesion was from the entire brain.

Table 1

Demographic information of the participants.

Characteristic	Control group	AD/MCI group
Number of subjects	10	16
Mean age ± S.D.	73.1 ± 4.4	70.7 ± 9.3
Gender		
Male	3	9
Female	7	7
Education (years) ± S.D.	14.8 ± 2.6	14.8 ± 3.2
MMSE score ± S.D.	28.7± 1.9	26.6 ± 3.5